Nonlinear Acoustics at GHz Frequencies in a Viscoelastic Fragile Glass Former

Christoph Klieber,[1,2,*] Vitalyi E. Gusev,[3,2] Thomas Pezeril,[2] and Keith A. Nelson[1,†]

[1]*Department of Chemistry, Massachusetts Institute of Technology, Cambridge, Massachusetts 02139, USA*
[2]*Institut Molécules et Matériaux du Mans, UMR-CNRS 6283, Université du Maine, 72085 Le Mans, France*
[3]*Laboratoire d'Acoustique de l'Université du Maine, UMR-CNRS 6613, Université du Maine, 72085 Le Mans, France*

Using a picosecond pump-probe ultrasonic technique, we study the propagation of high-amplitude, laser-generated longitudinal coherent acoustic pulses in the viscoelastic fragile glass former DC704. We observe an increase of almost 10% in acoustic pulse propagation speed at the highest optical pump fluence which is a result of the supersonic nature of nonlinear propagation in the viscous medium. From our measurement, we deduce the nonlinear acoustic parameter of the glass former in the gigahertz frequency range across the glass transition temperature.

The observation of laser-driven shock wave propagation provides direct experimental access to the equations of state of strongly compressed materials. This information is of paramount importance for geophysics, astrophysics [1], and inertial confinement fusion [2]. For many years, measurements of shock velocities have been possible through transit time measurements [3]. Only recently, single-shot optical velocity interferometry [2,4–9] allowed direct access to the dynamics of shock front motion in transparent solids but has been restricted to experimental configurations where the shock transforms the medium into a new, highly reflecting phase. Through this technique, the decay of both plane [4,7] and convergent [9,10] shocks with pressures exceeding tens of GPa have been reported. The propagation of shock waves in soft transparent materials such as polycarbonate and PMMA has been observed by single-shot ultrafast dynamic ellipsometry [11,12], a method allowing the separation of pressure-induced variations in elastic and optical properties. In such materials, characteristic pressures ranged from a few to 10–20 GPa, and acoustic Mach numbers defined as $M_A = u/v_0$, where u is the particle velocity and v_0 the linear acoustic velocity, were subsonic in the range $0.2 < M_A < 0.9$. Very recently, the propagation of weak shock waves with Mach numbers $M_A < 0.1$ and pressures below the damage threshold of the sample has been observed in thin sapphire slabs through ultrafast optical reflectivity [13], in a 4:1 methanol-ethanol mixture in a diamond anvil cell by ultrafast velocity interferometry [14], in a piezoelectric thin film through terahertz spectroscopy [15], and in a gold film through ultrafast plasmon interferometry [16] and ultrafast optical imaging [17]. In such weakly nonlinear acoustics experiments [18], no variation of the weak shock wave velocity during propagation has been reported to date. In a different manner, an indication for the nonlinearity of picosecond acoustic pulses with Mach numbers $0.0007 < M_A < 0.0018$ and their decay

within 1–3 mm propagation distances has been observed by classical Brillouin spectroscopy [19] through measurement of the distribution of 22 GHz longitudinal phonons along the acoustic pulse trajectory. In such experiments, information on wide-frequency-band nonlinear waves is obtained from the spatial distribution of a single Brillouin frequency component. The dependence of the Brillouin frequency shift on the amplitude or velocity of nonlinear acoustic pulses has been reported in one observation [20] of weak shock propagation in a solid sample.

In this Letter, we report direct measurements of the velocity of decaying, weak shock fronts in a glass-forming liquid using the technique of picosecond time-domain Brillouin scattering (TDBS) [21]. In liquids, this technique has been applied only to measurements of the propagation of linear acoustic pulses caused by the spatially inhomogeneous heating of a transducing material. In this work, we directly observe the decay of a weak shock wave as it propagates through the liquid sample. Our observations lead to an estimate of the nonlinear acoustic parameter of a fragile glass former [22] DC704 at around 20 GHz at temperatures across the glass transition.

Samples were prepared by squeezing liquid tetramethyl tetraphenyl trisiloxane (trade name DC704, glass transition temperature [23] $T_g \approx 210$ K, commonly used as diffusion pump oil) between two optically clear substrates, a generation side substrate which held a 33 nm aluminum transducer film and a detection side substrate. See the inset in Fig. 1(a). The liquid thickness was about 100 μm. Anhydrous DC704 was used as purchased from Sigma-Aldrich and forced through several linked 0.2 μm Teflon millipore filters to remove dust particles before applying to the sample without further purification. After the sample was assembled, it was transferred to a cryostat, and the sample chamber was immediately evacuated. Our front-back pump-probe setup was based on the common picosecond ultrasonics approach with TDBS detection [24–27].
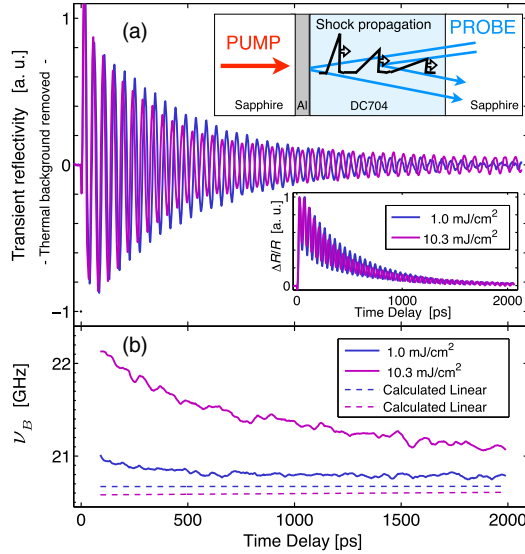
FIG. 1 (color online).   (a) Inset (top): Experimental setup with the ~100 μm liquid squeezed in between two sapphire substrates, one of them holding a 33 nm aluminum photoacoustic transducer film that launched an acoustic wave packet into the liquid through transient absorption of an optical pump pulse. Acoustic propagation in the liquid was then detected by a time-delayed optical probe pulse. (a) Inset (bottom): The propagating acoustic wave packet in the transparent liquid resulted in time-domain Brillouin scattering oscillations. There is also a nonoscillatory signal component due to thermally induced changes in reflectivity of the Al film. (a) Normalized data recorded at 200 K at two representative low and high fluences with thermoreflectance background removed. (b) Extracted values for the time variation of the "local" Brillouin frequency ν_B. Clearly apparent is the frequency down chirp with increasing time at high fluence caused by nonlinear acoustic propagation of the weak shock. The dashed lines show the calculated up chirp due to sample heating at 1.0 and 10.3 mJ/cm^2 pump fluence (top and bottom lines, respectively).

Absorption of an optical pump pulse and subsequent rapid thermal expansion launched the longitudinal acoustic wave packet into the sample. The excitation pulses from a Ti: sapphire amplifier laser system (Coherent RegA, 250 kHz repetition rate, 790 nm wavelength, 8 nm bandwidth, 200 fs pulse duration) were focused on the sample to a 100 μm spot. A small portion of the laser output was frequency doubled to 395 nm wavelength, time delayed to serve as a probe, and focused to a 40 μm spot at the sample.

Propagation of the acoustic waves from the transducer film into the liquid was optically detected by TDBS. The coherently scattered field, whose optical phase varied depending on the acoustic wave position, superposed with the reflected probe field from the metal transducer [Fig. 1(a), upper inset, illustrates the scattered and reflected components], resulting in signal intensity that showed time-dependent oscillations. The frequency ν_B of these oscillations is related as in any Brillouin scattering measurement to the propagation velocity v of the Fourier component ν_B

of the acoustic field and to the index of refraction n at the probe wavelength λ through the relation (in the case of normal incidence of the probe beam and 180° backreflection of the signal):

$$\nu_B = 2nv/\lambda. \tag{1}$$

Coherent Brillouin scattering data obtained at two different pump laser fluences are shown in Fig. 1(a). A nonoscillatory signal component due to thermoreflectance of the aluminum film (apparent in the lowest inset) has been subtracted to emphasize the acoustic signal components. The routine fitting procedure based on two damped exponents that we used to filter the thermal reflectance background did not influence the Brillouin component. After background removal, we fitted the whole time interval with an exponentially damped sinusoidal form to obtain a precise value of the mean Brillouin frequency. In a second step, we selected a short time window, about two and one-half oscillation cycles, and fitted it with an adjustable value for the Brillouin frequency ν_B, taking the mean Brillouin frequency as an input in the fit. We associated the obtained frequency with the middle value of the short time window. Shifting the time window by 10 ps increments, we repeated the second step over the whole available time delay between about 25 and 2000 ps, which allowed extraction of the time variation of the local Brillouin frequency. As a check on our procedure, we plotted the variable-frequency function determined by the successive fits and compared it to the data set. The fitted functions coincide almost exactly with the data set. Figure 1(b) shows the fitting results, the time evolution of the local Brillouin frequency. At the relatively low pump fluence of 1.0 mJ/cm^2, the acoustic strain amplitude is close to the limit of the linear response, and the Brillouin frequency is therefore almost constant over the recorded time delay interval. On the other hand, at about 10 times higher pump fluence of 10.3 mJ/cm^2, the initial Brillouin scattering frequency is significantly higher than in the low pump fluence limit and decreases with increasing time delay. This Brillouin frequency down chirp is a result of nonlinear acoustic effects and cannot be related to the heat flow into the liquid. From the temperature-dependent refractive index of DC704 at 395 nm, $n(T) = 1.748 - 4.9 \times 10^{-4}$ K$^{-1} \times T$ [K] [28], a temperature increase results in a decrease of n and therefore in a decrease of the Brillouin frequency with increasing laser fluence. Similarly, a temperature increase induces a decrease in the acoustic speed $v(T)$ of DC704 [28] that would also decrease the Brillouin frequency. We believe the only significant effects of the excitation laser pulse on the liquid sample are heating and acoustic wave generation, both mediated through direct contact with the Al layer that absorbs the laser light, and the results for $n(T)$ and $v(T)$ demonstrate that we can exclude temperature changes as

the origin of the fluence-dependent increase in Brillouin frequency shift that we observe. Careful finite element simulations of heating effects [29] in the sample, both on a single-shot basis (femtosecond to picosecond time scales) and steady state, were carried out in order to weight the influence of the temperature with respect to the nonlinear acoustic phenomena and to improve the quantitative analysis of the measured Brillouin frequencies. Our simulations of the heat diffusion reveal that the efficient heat flow into the sapphire allowed rapid cooling of the temperature rise at the laser-excited aluminum-sapphire interface to just 10% of its initial value (which could be as large as several hundred Kelvin) after ∼30 ps. In addition, single-shot heat flow into the liquid trails the acoustic wave and therefore could not influence its speed on a single-shot basis. Thus, based on our simulations, single-shot heat flow into the liquid had no detectable effect on the Brillouin scattering signal. In contrast, cumulative heating caused a nearly homogenous temperature rise of up to 4.5 K at the highest pump fluence of 10.3 mJ/cm^2 in the region of the liquid that included the propagating shock wave, according to the thermal modeling results. From the temperature-dependent refractive index of DC704 at 395 nm, and from the temperature-dependent speed of sound of DC704 [28], we calculated the change in Brillouin frequency in the linear acoustic regime due to laser heating according to Eq. (1). This resulted in a slight decrease in the linear Brillouin frequency with increasing fluence, as shown in Fig. 1(b). This slight correction of the linear Brillouin frequency enables quantitative comparison between the nonlinear and linear acoustic regimes at different laser fluences, as measured by TDBS.

In the nonlinear acoustic regime, the laser-excited acoustic pulse behaves as a weak shock wave with its characteristic strain profile, theoretically predicted as indicated in Fig. 1(a) to have, shortly after generation, a triangular form with a nearly instantaneous rise (the shock front) and a trailing edge of far longer duration. The peak amplitude is predicted to diminish and the duration to increase (maintaining constant integrated strain) during propagation [18]. The shock speed increases with increasing pressure, and, since in our experiment the pressure increases with the pump laser fluence, the Brillouin frequency shift increases as well. Because of nonlinear interactions among the spectral components of the wide-bandwidth weak shock pulse, the high-frequency components, including the selected Brillouin frequency, become preferentially spatially localized at the vicinity of the shock front. These spectral components give rise to the nonlinear steepening of the shock front, while the lower-frequency components are concentrated in the slower trailing edge [18]. Consequently, and as discussed theoretically [30], the velocity of the Brillouin frequency component detected through TDBS matches the velocity of the weak shock front.

A full set of transient reflectivity data covering a broad fluence range from 0.29 to 10.3 mJ/cm^2 were acquired and analyzed. From the extracted local Brillouin frequency time variation $\nu_B(t)$, we calculated the fractional Brillouin frequency shift $\Delta\nu_B(t)/\nu_B^\circ$, where $\Delta\nu_B(t) = \nu_B - \nu_B^\circ$ is the Brillouin frequency increase over the linear limit Brillouin frequency ν_B°. See Fig. 2. On the basis of the relationship between the Brillouin frequency and the velocity of the weak shock front discussed above [30], the fractional Brillouin frequency shifts of Fig. 2(a) can be modeled by the well-established analytical solution for nonlinear transformation of triangular shocks [18], which leads to

$$\frac{\Delta\nu_B(t)}{\nu_B^\circ} = \frac{\varepsilon M_A/2}{\sqrt{1 + (\varepsilon M_A/2)t/\tau_A}}, \qquad (2)$$

where ε is the nonlinear acoustic parameter and M_A the Mach number. Equation (2) assumes compressive strain acoustic pulses of triangular shape with duration τ_A and a δ-localized leading shock front formed well before the start of the 100–2000 ps measurement window, without significant broadening of the front throughout the window. Theoretical consideration of our sample and experimental conditions [30] indicated that for excitation fluences of 4.4 mJ/cm^2 and above these assumptions should be valid, in which case our signals arise selectively from the shock
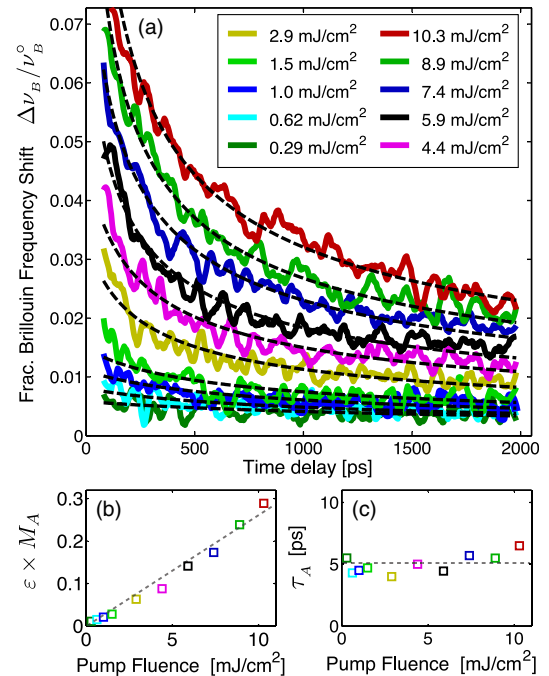

FIG. 2 (color online).   (a) Measured results of the fractional Brillouin frequency shift in DC704 for different laser pump fluences at 200 K sample temperature. Dashed lines are fits by Eq. (2). (b),(c) Fitting parameters $\varepsilon \times M_A$ and τ_A. Dashed lines are linear fits of the extracted parameters.

fronts. At progressively lower excitation fluences, Eq. (2) is valid for progressively shorter time periods. This may explain the poorer fits to data with fluences of 1.5 mJ/cm^2 and below, although the SNR levels are lower, since the signals were weaker.

The reduction of $\Delta \nu_B(t)$ with time in Eq. (2) is due to the decrease of the propagating weak shock front amplitude $\sim 1/\sqrt{1+(\varepsilon M_A/2)t/\tau_A}$ due to acoustic absorption which tends to dissipate the nonlinear steepening of the weak shock front [18]. The strongly nonexponential reduction of the frequency shift with time given by Eq. (2) is followed well by our results with excitation fluences of 2.9 mJ/cm^2 and higher over the complete experimental time window, as shown by the fits (with fitting parameters εM_A and τ_A) in Fig. 2(a). Thus, both the positive direction of our observed Brillouin shifts and their time-dependent evolution are consistent with a nonlinear acoustic origin. The approximately linear dependence of εM_A on fluence, as shown in Fig. 2(b), can be used to evaluate the nonlinear acoustic parameter of the liquid at the gigahertz frequency. Since the Mach number M_A scales linearly with fluence, our results indicate that the nonlinear parameter ε does not vary with fluence and can be assumed to be constant in the fluence range up to 10 mJ/cm^2. The mean value $\tau_A \simeq 5.2$ ps in Fig. 2(c) determined from the fits is in excellent agreement with the theoretically expected $\tau_A \simeq 5$ ps equal to the time of sound propagation through the aluminum film, providing an additional argument in support of the model expressed by Eq. (2).

Measurements of nonlinear acoustic parameters around a glass transition have never been reported at gigahertz frequencies. However, we can expect that, at the transition from the glass state to the highly viscous state, the acoustic nonlinearities may show a significant change due to the large-scale structural reorganization that becomes possible in the viscous liquid. In order to check this general expectation, we performed temperature-dependent TDBS measurements around the DC704 glass transition temperature at 2.9 mJ/cm^2 pump fluence. The results of temperature variation of the fitting parameter εM_A based on Eq. (2) are shown in Fig. 3(a). In order to extract the relevant ε parameter, we calculated the temperature-dependent Mach number M_A from the following equation:

$$M_A = \frac{4v/v_l}{(1+\frac{\rho_l v_l}{\rho v})(1+\frac{\rho v}{\rho_s v_s})} \times \beta \frac{\alpha F_L}{\rho C_p H}, \qquad (3)$$

where v, v_s, and v_l are the speeds of sound and ρ, ρ_s, and ρ_l the densities of aluminum, sapphire, and DC704, respectively, C_p is the heat capacity of aluminum, H is the aluminum thickness, β is the linear thermal expansion coefficient, α is the optical absorption coefficient for aluminum at 790 nm pump wavelength, and F_L is the laser fluence. The second multiplier on the right-hand side of Eq. (3) expresses the laser-generated strain,

while the first multiplier is related to the acoustic transmission and reflection across the aluminum-DC704 and aluminum-sapphire interfaces. The calculation was performed with temperature-dependent values for the coefficients from Refs. [28,31–33]. Finally, from the calculated weakly temperature-dependent M_A values displayed in Fig. 3(b), we have obtained the temperature evolution of the nonlinear coefficient ε across the glass transition temperature T_g, shown in Fig. 3(c). As expected, the nonlinear coefficient of the glass state is lower than of the viscous liquid state. The nonlinear coefficient increases in the liquid state about tenfold with a temperature increase of 50° above T_g. Over this same temperature range, the structural relaxation time scale for DC704 changes from seconds to microseconds [28]. However, those results and almost all other supercooled liquid dynamics measured to date describe the linear-response regime only. The nonlinear parameter may provide unique insight into the dynamics of structural rearrangements on a larger scale. Our measurements highlight a significant change of the acoustic nonlinearities across T_g, much more pronounced than for the linear acoustic parameters such as the gigahertz-frequency speed of sound that changes only by 10% for an equivalent temperature change [28]. The huge change in the nonlinear coefficient across T_g has similarities with results reported in ferroelectric ceramics [34] in which the nonlinear acoustic parameter at 10 MHz frequency diminished about 10 times when the temperature was reduced by 100° from the Curie temperature. The rise in ε with temperature above T_g is likely due in part to thermal energy reaching anharmonic regions of local intermolecular potentials, all the way to barrier heights
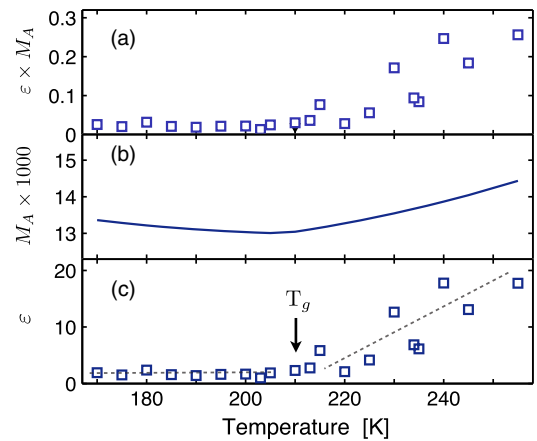

FIG. 3 (color online). Parameter values from fits to temperature-dependent results at 2.9 mJ/cm^2 pump fluence: (a) Extracted nonlinear parameter times acoustic Mach number $\varepsilon \times M_A$, where the theoretical and experimental value of $\tau_A = 5$ ps was used. (b) Calculated initial Mach number as a function of temperature and (c) corresponding nonlinear parameter ε versus temperature across the DC704 glass transition temperature $T_g \approx 210$ K. Dashed lines serve as guides to the eye.

that enable structural relaxation to occur at measurable rates. Measurement of the nonlinear response over a wide range of frequencies and sample temperatures will provide unique insights, beyond what can be deduced from the linear response spectrum, into the structural dynamics that are required for liquid flow and other large-scale rearrangements to occur.

We have measured acoustic amplitude-dependent Brillouin frequency shifts whose behavior is consistent with classical models of nonlinear acoustics. From our measurements we have extracted a material-specific non-linear acoustic parameter which in a solid characterizes the anharmonicity of the intermolecular interaction potentials and in a liquid should reflect the additional nonlinearity arising from structural relaxation. We determined the dependence of the nonlinear acoustic parameter of the fragile glass former DC704 at around 20 GHz at temperatures across the glass transition in the glass state and highly viscous and lightly viscous liquid states. Our technique opens the door to versatile measurements of gigahertz nonlinear acoustic phenomena of many materials and is especially suited to study disordered and partially ordered systems such as supercooled liquids, glasses, and colloidal suspensions [35] and ferroelectrics in which structural relaxation plays an important role.

---

*klieber@mit.edu
Present address: EP Schlumberger, 1 rue Henri Becquerel, 92140 Clamart, France.
†kanelson@mit.edu

[1] F. D. Stacey and P. M. Davis, *Physics of the Earth* (Cambridge University Press, Cambridge, England, 2008).

[2] G. W. Collins, L. B. Da Silva, P. Celliers, D. M. Gold, M. E. Foord, R. J. Wallace, A. Ng, S. V. Weber, K. S. Budil, and R. Cauble, Science **281**, 1178 (1998).

[3] M. D. Knudson, M. P. Desjarlais, and D. H. Dolan, Science **322**, 1822 (2008).

[4] P. M. Celliers, G. W. Collins, L. B. Da Silva, D. M. Gold, and R. Cauble, Appl. Phys. Lett. **73**, 1320 (1998).

[5] A. Benuzzi-Mounaix, M. Koenig, J. M. Boudenne, T. A. Hall, D. Batani, F. Scianitti, A. Masini, and D. Di Santo, Phys. Rev. B **60**, R2488 (1999).

[6] D. K Bradley, J. H. Eggert, D. G. Hicks, P. M. Celliers, S. J. Moon, R. C. Cauble, and G. W. Collins, Phys. Rev. Lett. **93**, 195506 (2004).

[7] A. Ravasio, G. Gregori, A. Benuzzi-Mounaix, J. Daligault, A. Delserieys, A. Ya. Faenov, B. Loupias, N. Ozaki, M. Rabec le Gloahec, T. A. Pikuz, D. Riley, and M. Koenig, Phys. Rev. Lett. **99**, 135006 (2007).

[8] S. Root, R. J. Magyar, J. H. Carpenter, D. L. Hanson, and T. R. Mattsson, Phys. Rev. Lett. **105**, 085501 (2010).

[9] T. R. Boehly, V. N. Goncharov, W. Seka, M. A. Barrios, P. M. Celliers, D. G. Hicks, G. W. Collins, S. X. Hu, J. A. Marozas, and D. D. Meyerhofer, Phys. Rev. Lett. **106**, 195005 (2011).

[10] T. Pezeril, G. Saini, D. Veysset, S. Kooi, P. Fidkowski, R. Radovitzky, and K. A. Nelson, Phys. Rev. Lett. **106**, 214503 (2011).

[11] S. D. McGrane, D. S. Moore, and D. J. Funk, J. Appl. Phys. **93**, 5063 (2003).

[12] C. A. Bolme, S. D. McGrane, D. S. Moore, and D. J. Funk, J. Appl. Phys. **102**, 033513 (2007).

[13] P. J. S. van Capel and J. I. Dijkhuis, Appl. Phys. Lett. **88**, 151910 (2006).

[14] M. R. Armstrong, J. C. Crowhurst, E. J. Read, and J. M. Zaug, Appl. Phys. Lett. **92**, 101930 (2008).

[15] M. Armstrong, E. Reed, K.-Y. Kim, J. Glownia, W. Howard, E. Piner, and J. Roberts, Nat. Phys. **5**, 285 (2009).

[16] V. Temnov, C. Klieber, K. A. Nelson, T. Thomay, V. Knittel, A. Leitenstorfer, D. Makarov, M. Albrecht, and R. Bratschitsch, Nat. Commun. **4**, 1468 (2013).

[17] T. Pezeril, C. Klieber, V. Shalagatskyi, G. Vaudel, V. Temnov, O. G. Schmidt, and D. Makarov, Opt. Express **22**, 4590 (2014).

[18] *Theoretical Foundations of Nonlinear Acoustics*, edited by O. Rudenko, and S. Soluyan (Consultants Bureau, New York, 1977).

[19] O. L. Muskens and J. I. Dijkhuis, Phys. Rev. Lett. **89**, 285504 (2002).

[20] A. Bojahr, M. Herzog, D. Schick, I. Vrejoiu, and M. Bargheer, Phys. Rev. B **86**, 144306 (2012).

[21] C. Thomsen, H. T. Grahn, H. J. Maris, and J. Tauc, Phys. Rev. B **34**, 4129 (1986).

[22] C. A. Angell, Science **267**, 1924 (1995).

[23] B. Jakobsen, K. Niss, and N. B. Olsen, J. Chem. Phys. **123**, 234511 (2005).

[24] H. J. Maris, Sci. Am. **278**, 86 (1998).

[25] C. Morath, G. Tas, T. C.-D. Zhu, and H. J. Maris, Physica (Amsterdam) **219–220B**, 296 (1996).

[26] T. Pezeril, C. Klieber, S. Andrieu, and K. A. Nelson, Phys. Rev. Lett. **102**, 107402 (2009).

[27] C. Klieber, T. Pezeril, S. Andrieu, and K. A. Nelson, J. Appl. Phys. **112**, 013502 (2012).

[28] C. Klieber, T. Hecksher, T. Pezeril, D. H. Torchinsky, J. C. Dyre, and K. A. Nelson, J. Chem. Phys. **138**, 12A544 (2013).

[29] C. Klieber, Ph.D. thesis, MIT, 2010, http://hdl.handle.net/1721.1/57801.

[30] V. E. Gusev, J. Appl. Phys. **116**, 064907 (2014).

[31] Y. Takahashi, T. Azumi, and Y. Sekine, Thermochim. Acta **139**, 133 (1989).

[32] A. J. C. Wilson, Proc. Phys. Soc. London **53**, 235 (1941).

[33] D. F. Gibbons, Phys. Rev. **112**, 136 (1958).

[34] J. K. Na and M. A. Breazeale, J. Acoust. Soc. Am. **95**, 3213 (1994).

[35] J. Mattsson, H. Wyss, A. Fernandez-Nieves, K. Miyazaki, Z. Hu, D. R. Reichman, and D. Weitz, Nature (London) **462**, 83 (2009).